Title	Electro-optic and electro-absorptive modulations of AlGaAs/GaAs quantum well using surface acoustic wave
Author(s)	Choy, WCH; Li, EH; Weiss, BL
Citation	Journal Of Applied Physics, 1998, v. 83 n. 2, p. 858-866
Issued Date	1998
URL	http://hdl.handle.net/10722/42779
Rights	Creative Commons: Attribution 3.0 Hong Kong License

Electro-optic and electro-absorptive modulations of AlGaAs/GaAs quantum well using surface acoustic wave

Wallace C. H. Choy
School of Electronic Engineering, Information Technology and Mathematics, University of Surrey, Guildford, Surrey, GU2 5XH, United Kingdom

E. Herbert Li[a)]
Department of Electrical & Electronic Engineering, University of Hong Kong, Pokfulam Road, Hong Kong

Bernard L. Weiss
School of Electronic Engineering, Information Technology and Mathematics, University of Surrey, Guildford, Surrey, GU2 5XH, United Kingdom

(Received 2 June 1997; accepted for publication 12 October 1997)

The surface acoustic wave produced electron absorptive and electro-optic modulation in AlGaAs/GaAs quantum well structures are theoretically analyzed. The quantum well structures are optimized by maximizing the optical confinement of the modal field in the active region and the piezoelectric effect of surface acoustic wave on the quantum wells. The effect of penetration depth of the surface acoustic wave on the number (1–25 periods) of quantum wells, serving as the active region, is being studied. For 1–5 period structures, the quantum wells are designed on the top surface so that a strong piezoelectric effect can be obtained. For the 25-period structure, the quantum wells locate at a depth of two-thirds the acoustic-wave wavelength in order to obtain a uniform surface acoustic-wave-induced electric field. The results show that the single and five quantum well devices are suitable for absorptive modulation and optical modulation, respectively, while a general advantage of the 25-period quantum well modulator can shorten the modulation interaction length and increase the modulation bandwidth. The effective index change of these devices are at least ten times larger than the conventional surface acoustic wave devices. These results make the surface acoustic wave quantum well modulators more attractive for the development of acousto-optic device applications. [S0021-8979(98)04202-9]

I. INTRODUCTION

Surface Acoustic Wave (SAW) have been widely investigated in piezoelectric bulk materials including $LiNbO_3$ and GaAs, where the structures are homogenous[1] or multilayered.[2] Relatively a small amount of work have been reported on the interaction of SAW in III–V semiconductor quantum well (QW) structures.[3] In comparison to bulk materials, QWs are attractive for their excitonic optical properties.[4,5] Through the advantage of the quantum-confined Stark effect (QCSE), QWs are used for electro-absorptive and electro-optic modulators.[6,7]

Among the various applications of SAW, a number of acousto-optical signal processing functions including modulation,[8] beam deflection,[9] tunable filtering,[10] and spectrum analysis[11] have been developed. Most of these applications make use of a change of refractive index induced by the elasto-optic and electro-optic effects of SAW. Recently, the studies of absorptive modulation generated by SAW have also been initiated.[12] These indicates that both the absorption change and refractive index change induced by SAW are attractive in modulation devices.

SAW technology provides the advantages in the design of spatially distributed QWs optical systems such as two-dimensional spatial light modulators and optical correlators because SAW are suitable for inducing the required predetermined electric-field distribution.[12] Moreover, as compared to a conventional p-i-n electrical biased modulator,[6] no p^+ and n^+ buffers or cladding layers are needed in the acoustic devices. The main reason is that SAW is launched by a transducer far away from the interaction region of the optical and electrical fields. SAW also needs no metal contacts to cover the interaction region. These can minimize the unexpected doping in the active region and the damage in the device structure. Furthermore, SAW provides another degree of freedom which allows implantation of an enhanced Bragg modulator using the QW structures.[13] As a consequence, SAW have definite benefits in optoelectronic applications.

The electric field induced by SAW reduce nonuniformly with depth,[3] which is an obstacle in the development of high efficiency modulators typically with a large number of QWs in the active region. Moreover, the penetration depth of SAW is usually one SAW wavelength (λ_{SAW}) deep. Here we will tackle this problem by analyzing single QW, 5-period QW, and 25-period QW SAW modulators, all of which are within one λ_{SAW} deep.

In this article, a theoretically analysis of the waveguide type 100 Å/100 Å $Al_{0.3}Ga_{0.7}As$/GaAs modulators (optical and absorptive) by using SAW is presented. This study addresses the nonlinear SAW effects on the QWs optical properties (including absorption coefficient and refractive index), the effect of optical confinement to the modulation efficiency, and the design and optimization of a single-period, 5-period, and 25-period QW modulators. The comparison between these three structures are also made so that the re-

a)Electronic mail: ehli@eee.hku.hk

 0021-8979/98/83(2)/858/9/$15.00

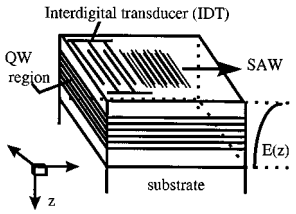

FIG. 1. Schematic diagram of the propagation of a SAW on top of QWs structure. $E(z)$ is the SAW-induced piezoelectric field amplitude, where z is the direction normal to the plane of the quantum wells.

sults can be used as a guideline to develop SAW-QW modulators.

II. MODELING THE SAW QUANTUM WELL MODULATORS

The waveguide type absorptive and optical modulators have an identical device structure and are shown schematically in Fig. 1. The layers, started from the substrate, consisted of an AlGaAs cladding, a stack of 100 Å $Al_{0.3}Ga_{0.7}As$ barriers and 100 Å thick GaAs wells which serves as the active region of the device, and a top cladding AlGaAs layer. One side of the device structure develops an interdigital transducer for launching the SAW.

In order to investigate these electro-absorption and electro-optic modulators, the SAW propagation and its piezoelectric and elastoelectric effects are modeled followed by their effects on the QW subband structure. The optical properties (absorption coefficient and refractive index) of these structures with the effects of excitons are then determined. In order to take into account the interaction of the optical waveguide field with the QW structure (which is tilted by the SAW induced field), a one dimensional Maxwell's equation is solved analytically. Subsequently, the change of both the effective absorption coefficient and the effective refractive index are calculated. Various performance parameters are then determined to characterize the modulation performance.

A. SAW model

The propagation of SAW is described by two equations. One is the motion equation of particles in elastic medium, which is given as

$$\frac{\partial T_{ij}}{\partial x_j} = \rho \frac{\partial^2 u_i}{\partial t^2}, \tag{1}$$

where T_{ij}, u_i and x_j are a components of the stress tensor, the particle displacement and the spatial direction, respectively, with the indices i and j labeling the spatial directions and summation over repeated indices has been implied. A second equation, shown below describes the electromagnetic wave properties of SAW, in which Maxwell's equations govern the electric fields and electric displacements of SAW. Under a quasi-static approximation, the electric displacement equation in a medium of no free charges is given as

$$\frac{\partial D_i}{\partial x_j} = 0, \tag{2}$$

where D is the electric displacement field. The method used to solve these two equations for a multilayered structures is described in Refs. 14 and 15. In order to obtain a high electromechanical coupling constant (to produce a large SAW amplitude) for structures such as GaAs and AlGaAs, the growth direction of the QW is $\langle 100 \rangle$ and the SAW propagates along the $\langle 110 \rangle$.[14]

B. QW optical parameters

It is assumed here that the barrier is thick enough that there is no significant coupling between adjacent wells and therefore a single QW model can be used here. The QW subband edge states in the Γ valley are calculated by an envelope function approximation,[16] using a Ben-Denial and Duke model,[17] resulting in an one-dimensional one particle Schrödinger-like equation for determining the electron and hole energy levels and envelope wave functions:

$$\frac{-\hbar^2}{2} \frac{d}{dz} \left[\frac{1}{m^*(z)} \frac{d}{dz} + V(z) \right] \chi_n(z) = E_n \chi_n(z), \tag{3}$$

where z denotes the growth direction, $V(z)$ is the confinement potential of QW, $m^*(z)$ is the effective mass of either the electron or holes, $\chi_n(z)$ represents the envelope wave function of either an electron or hole corresponding to the nth confined subband state with energy E_n.

A typical perturbation method is used to evaluate the SAW effects in the QW subband structure. SAW induces both strain and electric field in the AlGaAs/GaAs heterostructure, which is a piezoelectric material. However, the induced strains are small ($<0.1\%$) and are not large enough to modify the QW potential profile for a change of the semiconductor material band gap.[18] Consequently, only the SAW-induced electric field is considered as an extra linear perturbation term to $V(z)$ in modifying the QW potential profile. The transverse electric (TE) and transverse magnetic (TM) polarization dependent refractive index and absorption coefficients, including the contributions from the exciton, are determined. Details of the refractive index and absorption coefficient calculations can be found in Refs. 19 and 20, respectively. In our model, the refractive index is averaged for each QW period and the absorption coefficient is produced by the wells.

C. Optical properties of the SAW modulator

When an optical field propagates in the devices, only that portion which interacts with the QWs will be modulated due to the SAW effect. In order to calculate the optical properties (including the effective absorption coefficient and refractive index) of an acousto-optic QW modulator structure, a multilayer planar waveguide model is developed from our previous model[21] using the transfer matrix method. From this calculation, the modal field profiles and the propagation constants are obtained for the determination of the effective absorption coefficient and effective refractive index, respectively.

The effective absorption coefficient, α_{eff}, is given by

$$\alpha_{\text{eff}}=\frac{\int_{\text{the active region}}^{\text{the wells within}}\alpha(z)\varphi(z)\varphi^*(z)dz}{\int_{\text{of the guiding field}}^{\text{the entire cover range}}\varphi(z)\varphi^*(z)dz}, \tag{4}$$

where $\varphi(z)$ is the guiding optical field and $\alpha(z)$ is the material absorption coefficient of the QW structure. Since the amplitude of SAW varies with penetration depth, α is z dependent. Equation (4) shows that α_{eff} is determined by the fraction of the optical field intensity $\varphi(z)\varphi^*(z)$ within the wells of active region. The change of effective absorption coefficient $\Delta\alpha_{\text{eff}}$ of the device is calculated using

$$\Delta\alpha_{\text{eff}}=\alpha_{\text{eff}}(\text{SAW})-\alpha_{\text{eff}}(\text{no SAW}), \tag{5}$$

where α_{eff} (SAW) and α_{eff} (no SAW) are the effective absorption coefficients with and without SAW-induced electric field, respectively.

The effective refractive index of the structure, n_{eff}, is determined by solving Maxwell's equations for the waveguide using the material refractive indices. The change of the effective refractive index, Δn_{eff}, is calculated using

$$\Delta n_{\text{eff}}=n_{\text{eff}}(\text{SAW})-n_{\text{eff}}(\text{no SAW}), \tag{6}$$

where n_{eff} (SAW) and n_{eff} (no SAW) are the effective refractive indices with and without SAW-induced electric field, respectively.

D. Modulator performance

The important performance characteristics of the modulators are the modulation depth η for phase or diffraction modulation, the contrast ratio CR for absorptive modulation, optical confinement factor Γ, the chirp parameter β_{mod}, and the absorption loss α_{loss} for both modulations.

The modulation depth η indicates the efficiency of modulation due to the change of the effective index, such as diffraction and phase modulation, is given by

$$\eta=\sin^2(\Delta\phi/2), \tag{7}$$

where $\Delta\phi=2\pi/\Delta n_{\text{eff}}/\lambda_{\text{op}}$ is phase change, l is the SAW aperture, and λ_{op} is the operating optical wavelength. The SAW aperture for π phase change is commonly used to measure the phase modulation, the shorter the SAW aperture the larger the phase modulation can be obtained.

The contrast ratio CR is defined as the ratio of the light intensity with and without an SAW and is given by

$$\text{CR(dB)}=10\log\left(\frac{\exp[-\alpha_{\text{eff}}(\text{ON})l]}{\exp[-\alpha_{\text{eff}}(\text{OFF})l]}\right), \tag{8}$$

where α_{eff} (ON) and α_{eff} (OFF) are the effective absorption in the ON-state (no SAW-induced electric field) and the OFF-state (under SAW-induced electric field), respectively.

The static chirp parameter β_{mod} is given by

$$\beta_{\text{mod}}=\frac{4\pi\Delta n_{\text{eff}}}{\lambda_{\text{op}}\Delta\alpha_{\text{eff}}}, \tag{9}$$

where Δn_{eff} and $\Delta\alpha_{\text{eff}}$ are the change in the effective refractive index and the change in the effective absorption respectively. Equation (9) shows that β_{mod} can be considered as a measure of the ratio of the optical (refractive index) modulation strength to the optical intensity (absorption coefficient) modulation strength due to the SAW-induced electric field. Typical electro-optical (refractive index) and electro-absorptive types of modulator require a large than 10 and a less than 1 chirp parameters of >10 and <1, respectively.[22]

The optical confinement factor Γ is determined using

$$\Gamma=\frac{\int_{\text{the waveguide device}}^{\text{the core region of}}\varphi(z)\varphi^*(z)dz}{\int_{\text{of a guiding field}}^{\text{the entire cover range}}\varphi(z)\varphi^*(z)dz}, \tag{10}$$

where $\varphi(z)$ is the modal electric-field profile in the device structure and z is the growth direction of QW. This Γ parameter indicates the portion of the optical power overlapping with the core region, which is consisted of QWs active region and two buffer layers between QWs and two (top and bottom) cladding layers, within the entire device structure. Therefore, an efficient modulator requires a large value of Γ. High performance modulators also require low α_{loss}, which is a measure of the insertion loss of the device. For phase modulation, α_{loss} is defined as α_{eff} without the SAW effect when, for absorptive modulator, α_{loss} is defined as the ON-state α_{eff}.

III. RESULTS AND DISCUSSIONS

The three QW structures considered here are 1, 5, and 25 periods of an 100 Å/100 Å $Al_{0.3}Ga_{0.7}As$/GaAs QW structure. They are used as an active region of the acousto-absorptive and -optic modulators. It should be noted that a high performance absorptive modulator requires a high CR, a low optical modulation (and thus low β_{mod}), and a low α_{loss}. On the other hand, a good electro-optic modulator requires a high η, a large phase change, a low absorption change (and thus high β_{mod}), a short SAW aperture for π phase change and a low α_{loss}.

In the calculation of absorption coefficient, the Lorentzian broadening profile is used and the half width half maximum (HWHM) exciton broadening factor are extracted from experimental data.[23,24] The HWHM of the heavy hole (HH) and the light hole (LH) are considered to be the same and have a value of 3 meV which is averaged from the values taken from Refs. 24 and 25. It should be noted that although the piezoelectric electric field induced by SAW will enhance the broadening factor, its effect to the broadening factor is still not well known and this effect has not been considered in our model.

The effects of SAW on the QWs are first investigated. Through the understanding of optical guiding and interaction between the modal field and active region, a 5-period and a single QW modulators are then analyzed. In order to enhance the modulation efficiency and to reduce the SAW aperture (modulation length), an optimized QW modulator structure containing 25 QWs is designed and its performance is also addressed here.

A. SAW effects in QW structures

The effects of SAW, with power and wavelength of 10 mW and 2 μm, respectively, on the optical properties of 25-period of QWs structures on top of a thick $Al_{0.5}Ga_{0.5}As$ lower cladding layer is considered here. The QW potential profiles are tilted by a SAW-induced potential, as shown in

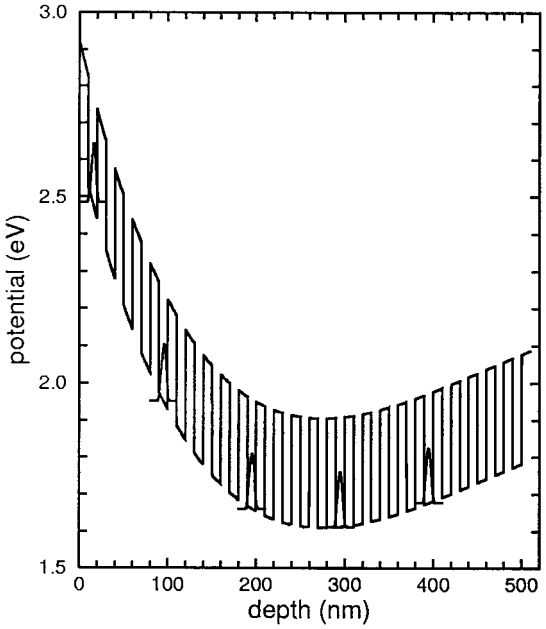

FIG. 2. 25 periods of QWs on top of $Al_{0.5}Ga_{0.5}As$ cladding tilted by SAW potential. The first wave function of the 25 periods of QWs localize in the well without serious tunneling.

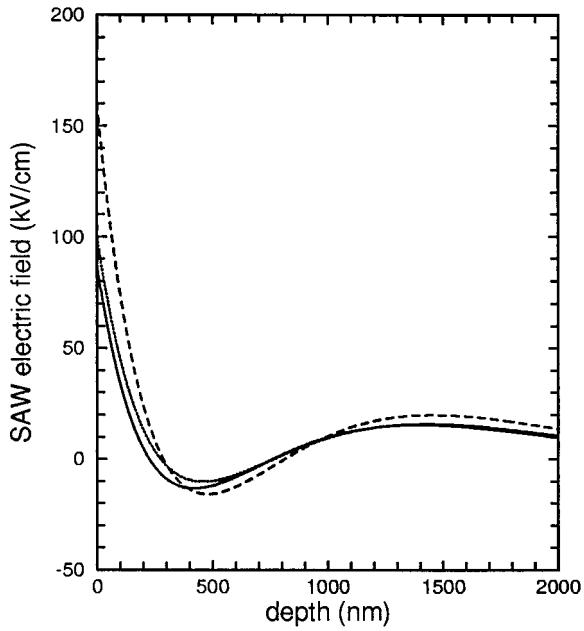

FIG. 4. SAW-induced electric field in different structure: 25 periods of QWs on top of $Al_{0.5}Ga_{0.5}As$ cladding (solid line), 5 periods of QWs on top of $Al_{0.5}Ga_{0.5}As$ cladding (dot line), and 5 periods of QWs on top of AlAs cladding (dash line).

Fig. 2. It can be observed that the slope of the QW potential profile reduces gradually and eventually slightly increases in the deeper QWs. The wave functions of the fundamental states over these 25 QWs are localized in the wells without significant tunneling between adjacent wells. The corresponding absorption spectra of this 25-QW structure is shown in Fig. 3. The quantum-confined Stark shift reduces with depth starting from the first quantum well since the gradient of QW potential profile reduces. The Stark shift between the 5th and 25th QW is so small that the exciton edges locate at almost the same wavelength as that of the QW exciton band edge without any SAW effect. Consequently, only the first 5 QWs (thickness equivalent to a depth of 0.05 λ_{SAW}) are suitable for use as a QCSE modulator.

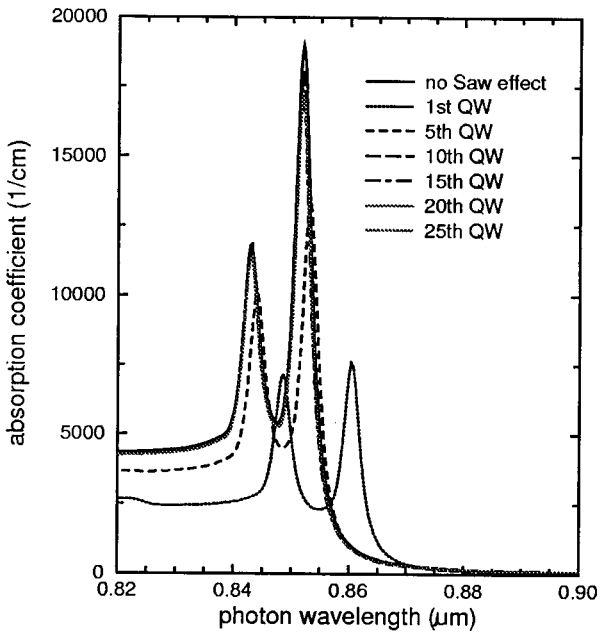

FIG. 3. TE mode absorption spectra of 25 periods of QWs on top of $Al_{0.5}Ga_{0.5}As$ cladding, no SAW effect (solid line): 1st QW (dot line), 5th QW (dash line), 10th QW (long dash line), 15th QW (dash-dotted line), 20th QW (light color solid line), 25th QW (light color dot line).

B. 5-period QW modulator

To develop the 5-QW structure as electro-optic and electro-absorptive modulators, the SAW effect has to be enhanced and the modal optical field has to be confined to these 5 QWs for optimizing the modulation efficiency. As shown in Fig. 4, the SAW-induced electric field can be increased by reducing the number of QWs from 25 to 5. This improvement can be enhanced further by increasing the Al composition of the lower cladding layer from $Al_{0.5}Ga_{0.5}As$ to AlAs. However, since the waveguide core region of 0.11 μm (5-QW) is too thin to support any guiding modes, an extra buffer layer of $Al_{0.5}Ga_{0.5}As$ is inserted between the QWs and lower cladding layer. By increasing the thickness of this buffer layer from 0 to 0.04 μm, the first guided mode is obtained. Therefore, the optimized structure contains a GaAs substrate, a 2 μm AlAs cladding layer, a 0.04 μm $Al_{0.5}Ga_{0.5}As$ buffer layer with 5 QWs on top. The SAW power and λ_{SAW} are 10 mW and 2 μm, respectively. The modal field and the refractive index profile of the structure at λ_{op}=0.872 μm are shown in Fig. 5. The lower number of QW periods and increment of Al composition improve the confinement of optical field to the QW region. As compared to the previous 25-QW structure, the optical confinement of the modal field in the top five QWs (thickness equivalent to

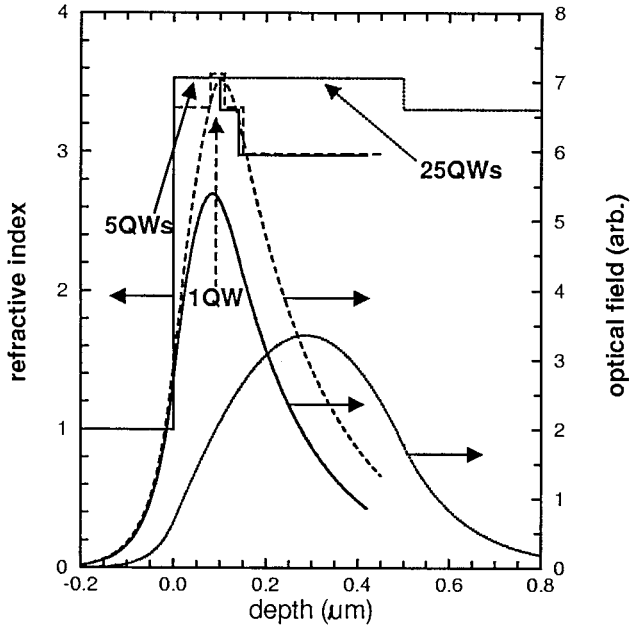

FIG. 5. Modal field and refractive index profile of different QWs structures: the 5 QWs modulators (solid line), the 25 QWs on top of of $Al_{0.5}Ga_{0.5}As$ cladding (dot line), the single QW modulator structure (dash line).

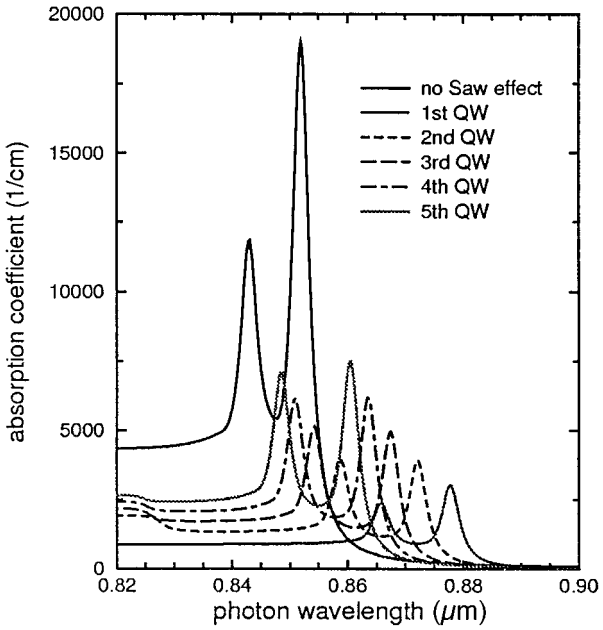

FIG. 6. TE mode absorption spectra of QWs in the 5 QWs modulator: QW without SAW effect (solid line), 1st QW (dot line), 2nd QW (dash line), 3rd QW (long dash line), 4th QW (dashed dot line), 5th QW (light color solid line).

$0.05\ \lambda_{SAW}$) improves by more than 40 times from less than 0.01 to 0.4 in the optimized structure which results in a higher modulation efficiency.

The absorption modulator is selected to operate at the wavelength of the HH exciton peak in the presence of a SAW. The TE mode absorption coefficient of the 5-QW structure is shown in Fig. 6. Although the exciton band edges of these 5 QWs do not coincide due to the decay of the SAW-induced electric field with depth, the magnitude of quantum-confined Stark shift of each of these QWs increases by comparing the first QW and the fifth QW to that of the previous 25-QW structure. This implies that the optimised structure is more practical for device applications. The electro-optic and electro-absorptive modulators of the 5-QW device are given in Table I. For the absorptive modulator, there is a tradeoff between $\Delta\alpha_{\text{eff}}$ (and thus CR) and α_{loss}. For instance, at $\lambda_{\text{op}}=0.852\ \mu$m, although $\Delta\alpha_{\text{eff}}$ is as high as $6000\ \text{cm}^{-1}$ (calculated from Fig. 6), but $\alpha_{\text{loss}}=1100\ \text{cm}^{-1}$ is too large to be practical. In order to have a lower α_{loss}, λ_{op} should be kept away ($\geqslant 0.86\ \mu$m) from the exciton absorption edge without the SAW effect. λ_{op} is selected to be 0.864 μm for an optimized absorptive modulation. For a SAW aperture of 500 μm, the CR, α_{loss}, and β_{mod} are 21.4 dB, $427.5\ \text{cm}^{-1}$ and -0.5, respectively. β_{mod} is negative at this wavelength, so that frequency compression of the optical source is possible which makes this modulator attractive.

For optical modulation, there are tradeoff's among refractive index change, α_{loss} and β_{mod}. As shown in Fig. 7, the change of refractive index maximizes at $\lambda_{\text{op}}=0.853\ \mu$m. At this optical wavelength, β_{mod} is less that 10 due to a large $\Delta\alpha_{\text{eff}}$ as shown in Fig. 6, and α_{loss} is large ($\geqslant 1000\ \text{cm}^{-1}$). Consequently, it is not practical to operate at this λ_{op}. It is

TABLE I. Modulation properties of the 5 QWs modulator. The SAW aperture is 500 μm.

Absorptive modulation					
λ_{op} (μm)	α_{loss} (cm^{-1})	$\Delta\alpha_{\text{eff}}$ (cm^{-1})	Δn_{eff} (10^{-2})	CR (dB)	β_{mod}
0.860	225.0	436.7	−1.27	21.8	−4.24
0.862	155.7	423.8	−6.36	21.2	−21.88
0.863	133.2	437.6	−4.01	21.9	−1.35
0.864	115.7	427.5	−0.50	21.4	−0.50
8.866	90.4	293.7	−0.45	14.6	−0.45

Phase modulation								
λ_{op} (μm)	α_{loss} (cm^{-1})	$\Delta\alpha_{\text{eff}}$ (cm^{-1})	n_{eff} (SAW)	n_{eff} (no SAW)	$\Delta\phi$ (rad)	η	l for $\Delta\phi=\pi$	β_{mod}
0.876	39.9	43.3	3.07548	3.07529	0.68	0.11	2305	0.62
0.878	35.6	49.7	3.07317	3.07246	2.54	0.91	618	2.04
0.880	32.1	16.6	0.07059	3.06983	2.71	0.95	579	6.54
0.881	30.5	7.3	3.06918	3.06859	2.10	0.75	746	11.5
0.882	29.1	2.0	3.06783	3.06739	1.56	0.50	1002	31.3

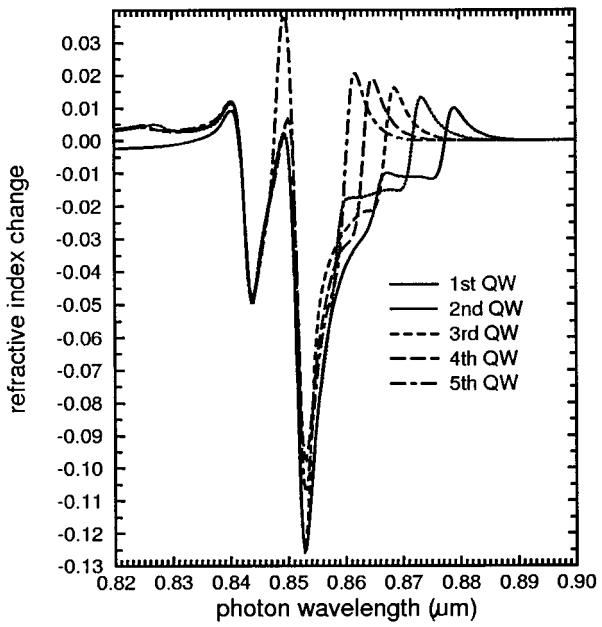

FIG. 7. TE mode refractive index spectra of QWs in the 5 QWs modulator: 1st QW (solid line), 2nd QW (dot line), 3rd QW (dash line), 4th QW (long dash line), 5th QW (dashed dot line).

useful to note that β_{mod} is >10, which is the requirement for a good phase modulator, for λ_{op} above 0.881 μm. The value of β_{mod} can be increased by operating at longer wavelength, however, there is a parasite of a weaker phase change as shown in Table I. As a consequence, the selected operating wavelength λ_{op} is above 0.881 μm, at where $\Delta\phi$ is 2.1 rad and α_{loss} is only 7.3 cm^{-1}.

C. Single QW modulator

In order to improve the absorption modulation to obtain a higher CR and lower α_{loss}, as compared to the previous 5-QWs case, a single QW structure is used. In the previous 5-QW structure the mode field peaks at ~0.1 μm and the thickness of the core region (including the buffer region) is the minimum thickness required to obtain a single mode operation. Consequently, the single QW structure is designed to put the QW at a depth of 0.1 μm and the thickness of the core for the single QW device is similar to that of the 5-QW structure. This will result in a strong overlapping between the mode field profile and the active region together with a well-confined single optical mode. The structure of the single QW modulator is a GaAs substrate, 2 μm AlAs lower cladding layer, 0.04 μm $Al_{0.5}Ga_{0.5}As$ buffer region, 100 Å/100 Å $Al_{0.3}Ga_{0.7}As$/GaAs single QW, and 0.08 μm upper $Al_{0.5}Ga_{0.5}As$ cladding layer. The power of SAW and λ_{SAW} are the same as those for the 5-QW structure. The refractive index profile and the modal field are shown in Fig. 5. As expected, the peak of modal line locates at the single QW region with only a slight mismatch. This is because λ_{op} is selected to be ~0.859 μm instead of 0.872 μm, as is used in the 5-QW structure. With a difference of λ_{op} the refractive index of the structure changes and thus produces an acceptable small shift of the modal field peak position.

The absorption modulator properties are given in Table II. For a SAW aperture of 500 μm, the CR is 17.8 dB and β_{mod} is −0.87 at a λ_{op} of 0.864 μm. This value of β_{mod} is negative so that frequency compression can be achieved. Although the Γ of this device reduces to 0.2, half that of the 5-QW structure, the modulation performance, in terms of α_{loss} and CR, is better than the 5-QW structure. The main reason is that, α_{loss} in the single QW device 71.6 cm^{-1}, which is only ~60% of that in the 5-QW structure at for a λ_{op} between 0.862 and 0.866 μm. For the same optical power loss, the CR of the single QW structure can be increased by more than seventeen times, i.e., ~124 dB, while that of 5-QW one is only 22.7 dB. In the single QW structure, only the QW contributes to α_{loss} and there is no absorption loss in the bulk AlGaAs cladding layers at such long λ_{op}. On the other hand, in the 5-QW case, due to the variation of the exciton edges of the 5 QWs, the fourth QW predominantly determines the absorption change of the optical field at the optimized λ_{op}=0.864 μm, while other QWs pro-

TABLE II. Modulation properties of the single QW modulator. The SAW aperture is 500 μm.

Absorptive modulation					
λ_{op} (μm)	α_{loss} (cm^{-1})	$\Delta\alpha_{\text{eff}}$ (cm^{-1})	Δn_{eff} (10^{-2})	CR (dB)	β_{mod}
0.859	71.6	356.8	−2.12	17.8	−0.87
0.86	57.6	351.0	3.21	17.5	1.34
0.861	47.4	112.5	−4.02	10.6	2.77
0.862	39.9	62.2	2.98	5.6	3.86
0.863	34.2	36.2	2.05	3.1	4.80

Phase modulation								
λ_{op} (μm)	α_{loss} (cm^{-1})	$\Delta\alpha_{\text{eff}}$ (cm^{-1})	n_{eff} (SAW)	n_{eff}(no SAW)	$\Delta\phi$ (rad)	η	l for $\Delta\phi=\pi$	β_{mod}
0.864	29.7	36.2	3.04840	3.04698	5.16	0.28	304	5.7
0.865	26.1	22.0	3.04644	3.04543	3.67	0.93	428	6.8
0.866	23.2	13.6	3.04462	3.04396	2.39	0.87	656	7.0
0.867	20.8	8.5	3.04287	3.04250	1.34	0.39	1171	6.3
0.868	18.8	5.2	3.04135	3.04109	0.94	0.21	1669	7.2
0.869	17.4	2.7	3.03994	3.03970	0.86	0.19	1810	12.9
0.870	15.7	1.5	3.03855	3.03833	0.79	0.15	1977	21.2

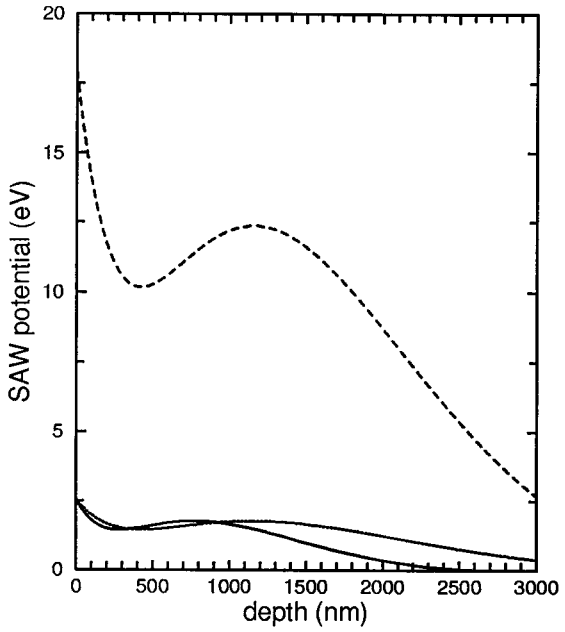

FIG. 8. SAW potential in different material structures: 25 QWs located at depth from 1.9 to 2.4 μm and SAW with 2 μm wavelength launched (solid line), the same structure and SAW with 3 μm wavelength launched (dot line), and the same structure with ZnO deposited on top and SAW with 3 μm wavelength launched (dash line).

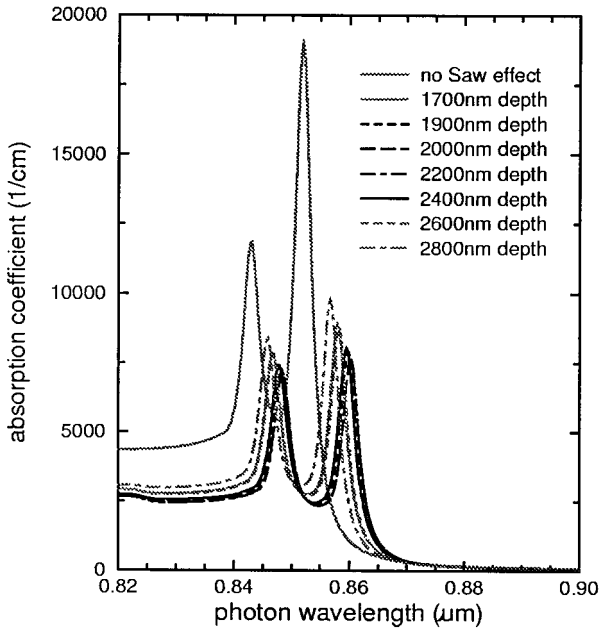

FIG. 9. TE mode absorption spectra of a QWs at different depth from 1.7 to 2.8 μm: a reference QW without any SAW effect (light solid line), QW at 1.7 μm (light dot line), QW at 1.9 μm (dashed line), QW at 2 μm (long dash line), QW at 2.2 μm (dashed dot line), QW at 2.4 μm (light dash line), and QW at 2.8 μm (light dashed dot line).

vide a weaker absorption change, as shown in Fig. 6. Moreover, at the optimized operating wavelength, all of the QWs provide the same amount of α_{loss} ($115.7\ \text{cm}^{-1}$) without any SAW-induced effects. These effects explain why the single QW structure has a better modulation performance than the 5-QW structure.

A λ_{op} of 0.869 μm is selected for the operating wavelength of the phase modulator since the optical modulation is larger in the region with $\beta_{\text{mod}} > 10$, as shown in Table II. When λ_{op} is reduced to 0.866 μm, a larger phase change of 2.39 rad can be obtained but β_{mod} is relative weak, 7. By comparing the modulation performance in terms of phase change, for the same power loss, this single QW device is 1.52 rad at the selected λ_{op}, which is weaker than that of the 5-QW structure at λ_{op} of 0.882 μm. Consequently, the 5-QW modulator provides a better phase modulation, while the single QW structure is better for absorption modulation.

D. 25-period QW modulator

There are two important factors in the development of a SAW modulator with 25-period ($\sim$0.5 μm) QW active region. Firstly, a linear SAW-induced potential over a depth of 0.5 μm is required so that consistent exciton absorption edges can be obtained. Secondly, a large SAW potential gradient $\geqslant$50 kV/cm is required so that a large enough QCSE can be produced. As shown in Fig. 8, a more linear SAW-induced potential is obtained by increasing λ_{SAW} from 2 μm (solid line) to 3 μm (dot line). However, the SAW potential is too weak to provide the required QCSE. A 0.3 λ_{SAW} thick layer of ZnO deposited on the top surface of the AlGaAs/GaAs material structure may be used to enhance the SAW-induced potential by a factor of 7.[25] A linear SAW potential, with gradient equivalent to an applied electric field of $\sim$80 kV/cm, can therefore be obtained at depths between 1.7 and 2.8 μm; a range greater than 0.5 μm.

The absorption spectra of QWs at different depths are shown in Fig. 9. The strength of the QCSE in depths ranged from 1.9 μm (equivalent to a depth of 2/3 λ_{SAW} to 2.4 μm is quite consistent so that the exciton absorption edges of respectively QWs coincide at the same photon wavelength. Consequently, a modulator with a 25-QW can be designed to have useful modulator properties. The structure consists of a GaAs substrate, a 2 μm $Al_{0.5}Ga_{0.5}As$ lower cladding layer, 25 periods of $Al_{0.3}GaAs/GaAs$ QWs, 1.9 μm of $Al_{0.5}Ga_{0.5}As$ of upper cladding layer and a ZnO film on top to enhance the SAW potential. The power of SAW and λ_{SAW} are 10 mW and 3 μm, respectively. The refractive index profile and the modal field of this device structure for $\lambda_{\text{op}}=0.86$ μm are shown in Fig. 10. Since the core thickness has increased from $\sim$0.14 μm in previous two structures to 0.5 μm in the 25-QW structure here, the optical confinement factor of this structure is over 0.92.

The λ_{op} for the absorption modulator should be in the range between 0.859 and 0.861 μm. Since all HH exciton peaks of the 25 QWs, in the present of the SAW, merge with in this wavelength range, a large absorption change can be obtained. Moreover, a negative refractive index change can be achieved in the region between 0.859 and 0.86 μm so that a negative β_{mod} and thus frequency compression can be produced, see Fig. 11. The properties of the absorption modulator in this optical wavelength range are given in Table III. For a SAW aperture of 50 μm, β_{mod} and CR are -0.17 and 15.2 dB, respectively for λ_{op} of 0.86 μm. For optical modulation, as shown in Fig. 11, variations of the material refrac-

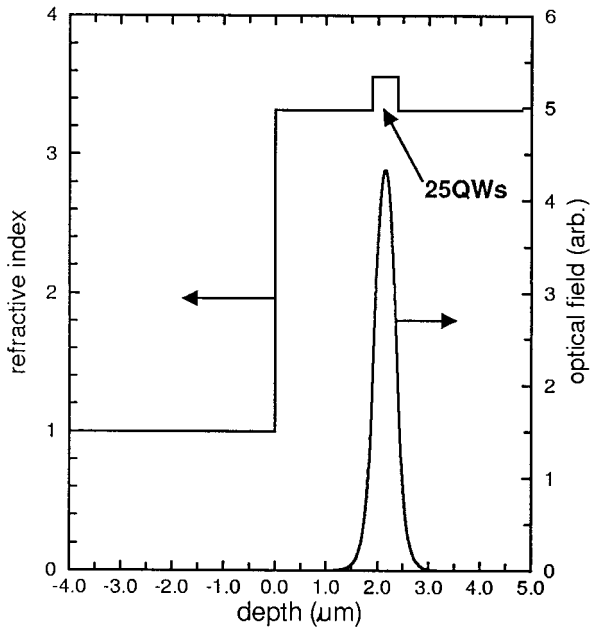

FIG. 10. Modal field and refractive index profile of the 25 QWs modulators.

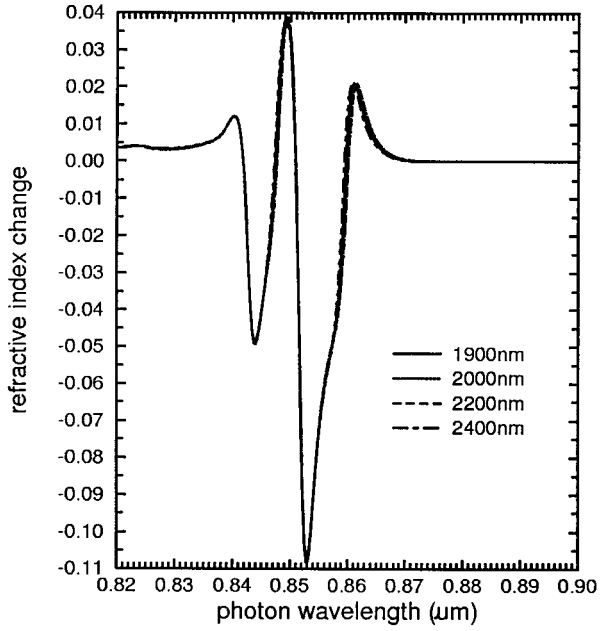

FIG. 11. TE mode refractive index spectra of QWs in the 25 QWs modulator: QW at 1.9 μm (solid line), QW at 2 μm (dot line), QW at 2.2 μm (dash line), and QW at 2.4 μm (long dashed line).

tive index change with wavelength is almost the same in comparison to the 5-QW structure where the curves do not coincide as shown in Fig. 7. For a SAW aperture of 50 μm, one-tenth of the 5-QW structure, at a selected λ_{op} of 0.870 μm, the phase change is >0.51 rad and η is above 6.3 for a β_{mod} of 10.8. The refractive index change for a bulk AlGaAs SAW modulator is $\sim 10^{-4}$,[26] while it is $\sim 10^{-3}$ in our optical modulator, as given in Table III. This implies that the optical modulation obtained here is an order of magnitude better than a conventional bulk III–V semiconductor SAW device. For both electro-optic and electro-absorption modulators, since the number of QW periods increases to 25, the SAW aperture can be reduced from 500 to 50 μm, while the CR retains the same order of magnitude. Therefore, the interaction time between the mode field and the SAW reduces, which implies that the modulator bandwidth also increases in the 25-QW structure.

IV. CONCLUSIONS

SAW produce electro-absorptive and electro-optic modulations in QWs have been investigated theoretically. The QW active region including 100 Å $Al_{0.3}Ga_{0.7}As/GaAs$ single QW, 5 periods QW and 25 periods QW. Since the SAW effects reduce nonuniformly with depth in these structures, the location of the QW stack and its number of period need to be designed and optimized carefully. Our results show that the active QW region with a thickness less than 5% of λ_{SAW} should best be placed at the top surface so that strong SAW effects can be utilized. For a thick QW structure, such as 25-period QW, an uniform SAW-induced electric field is required and therefore the period QW should be is located at a depth of $\sim 2/3\ \lambda_{SAW}$ below the top surface where the SAW-induced field is of a lower magnitude. Since the SAW potential in this region is small, deposited ZnO

TABLE III. Modulation properties of the 25 QWs modulator. The SAW aperture is 50 μm.

Absorptive modulation					
λ_{op} (μm)	α_{loss} (cm^{-1})	$\Delta\alpha_{eff}$ (cm^{-1})	Δn_{eff} (10^{-2})	CR (dB)	β_{mod}
0.859	644.5	2041	−3.0	10.2	−2.14
0.86	520.5	3029.5	−3.48	15.2	−0.17
0.861	431	2585	1.83	12.9	1.03

Phase modulation								
λ_{op} (μm)	α_{loss} (cm^{-1})	$\Delta\alpha_{eff}$ (cm^{-1})	n_{eff} (SAW)	n_{eff} (no SAW)	$\Delta\phi$ (rad)	η	l for $\Delta\phi=\pi$	β_{mod}
0.869	162.6	36.1	3.48234	3.48079	0.56	7.64	280	6.2
0.870	149.7	18.9	3.48001	3.47860	0.51	6.34	308	10.8
0.871	138.6	7.1	3.47781	3.47654	0.46	5.15	343	25.8

films are required to enhance the SAW-induced potential. Moreover, longer λ_{SAW} are used to obtain a more linear SAW potential. Optical confinement of the active region is shown to be important for the high modulation efficiency. For modulation with thin active QW region, such as single and five periods QW, high Al concentration cladding layers should be used.

From the modulation properties of the three QW periods, it is concluded that the single QW structure provides better absorption modulation than the 5-QW structure, while it is vice verses for the optical modulation. The 25-QW modulators offer the advantage of a smaller SAW aperture, and thus higher modulation bandwidth can be achieved as compared to the other two smaller QW structures. By comparison with conventional SAW devices, the effective index change of these SAW-QW devices provide at least a ten times improvement. Consequently, using SAW to produce large electro-optic and electro-absorptive modulations makes the acousto-absorptive and acousto-optic devices much more attractive than the bulk or heterojunction structures for SAW applications.

ACKNOWLEDGEMENTS

This research work is supported by the Hong Kong RGC earmarked grant. One of the authors (W. C. H. Choy) acknowledges financial support from the Croucher Foundation.

[1] C. S. Tai, *Guided-Wave Acousto-Optics: Interaction, Devices and Applications* (Springer, New York, 1990), Chap. 5.
[2] W. J. Tanski, S. W. Merritt, P. N. Sacks, D. E. Cullen, E. J. Branciforte, R. D. Carroll, and T. C. Eschrich, Appl. Phys. Lett. **52**, 18 (1988).
[3] F. C. Jain, and K. K. Bhattacharjee, IEEE Photonics Technol. Lett. **1**, 307 (1989).
[4] D. S. Chemla, T. C. Damen, D. A. B. Miller, A. C. Gossard, and W. Wiegmann, Appl. Phys. Lett. **42**, 864 (1983).
[5] D. A. B. Miller, D. S. Chemla, T. C. Damen, A. C. Goddard, W. Wiegmann, T. H. Wood, and C. A. Burrus, Phys. Rev. B **32**, 1143 (1985).
[6] T. H. Wood, J. Lightwave Technol. **6**, 743 (1988).
[7] Y. Kas, H. Nagai, M. Yamaniahi, and I. Suemune, IEEE J. Quantum Electron. **23**, 2167 (1987).
[8] M. Hatori, H. Muira, H. Sunagawa, M. Takeuchi, and K. Yamanoushi, Jpn. J. Appl. Phys., Part 1 **32**, 3467 (1993).
[9] J. Chang, N. Harada, and S. Kashiwa, Electron. Lett. **23**, 1384 (1987).
[10] C. D. Tran and M. Bratelt, Rev. Sci. Instrum. **63**, 2932 (1992).
[11] Y. Abdelarzek and C. S. Tsai, J. Lightwave Technol. **8**, 1833 (1992).
[12] T. Gryba and J. E. Lefevra, IEE Proc.: Optoelectron. **141**, 62 (1994).
[13] F. C. Jain, K. K. Bhattacharjee, and T. W. Groudkowki, *Proc. IEEE Ultrasonics Symposium* (IEEE Service Center, Lake Buena Vista, 1991), p. 529.
[14] Y. Kim and W. D. Hunt, J. Appl. Phys. **68**, 4933 (1990).
[15] C. Thompson and B. L. Weiss, J. Appl. Phys. **78**, 5002 (1995).
[16] G. Bastard and J. A. Brum, IEEE J. Quantum Electron. **22**, 113 (1987).
[17] D. J. Ben-Daniel and C. B. Duke, Phys. Rev. **152**, 683 (1966).
[18] A. R. Adams and D. J. Dunsan, Semicond. Sci. Technol. **5**, 1194 (1990).
[19] E. H. Li, B. L. Weiss, K. S. Chan, and J. Micallef, Appl. Phys. Lett. **62**, 550 (1993).
[20] W. C. H. Choy, E. H. Li, and J. Micallef, IEEE J. Quantum Electron. **33**, 1316 (1997).
[21] W. C. H. Choy and E. H. Li, IEEE J. Quantum Electron. **33**, 382 (1997).
[22] T. Hausken, R. H. Yan, R. I. Simes, and L. A. Coldren, Appl. Phys. **55**, 718 (1989).
[23] J. Singh, S. Hong, P. K. Mhatacharya, R. Sahai, C. Lastufka, and H. R. Sobel, J. Lightwave Technol. **6**, 818 (1988).
[24] T. Hayakawa, K. Takahashi, M. Kondo, T. Suyama, S. Yamamoto, and T. Hijikata, Phys. Rev. Lett. **60**, 349 (1988).
[25] Y. Kim and W. D. Hunt, J. Appl. Phys. **71**, 2136 (1992).
[26] R. G. Hunsperger, *Integrated Optics, Theory and Technology* (Springer, New York, 1985), Chap. 9.